Plexus brachialis Strain and Compression Deformation in the Costo-Axillary-Brachial Region: A Cadaveric Study

Edgars Vasilevskis[1], Sandra Skuja[2], Irina Evansa[1], Eva Šteina[1], Anna Sondore Pīlipa[1], Grigorijs Vābels[3], Uldis Teibe[4], Haralds Jansons[5], Valērija Groma[2], Indulis Vanags[1]

[1]Department of Anesthesiology, Riga Stradins University, Latvia,
[2]Department of Histology, Riga Stradins University, Latvia, [3]State Forensic Medicine Center, Riga, Latvia,
[4]Department of Physics, Riga Stradins University, Latvia, [5]Riga Stradins University, Latvia

Key words: *postoperative neuropathy; plexus brachialis; strain deformation; compression deformation.*

Summary. *Objective. The aim of this study was to clarify the role of different mechanisms in nerve injury during arm abduction positions. The tasks were to determine the strain deformation of the plexus brachialis during arm abduction, to measure the pressures in the neurovascular bundle in the cervico-costoclavicular-axillary area, and evaluate the histological changes of nerve after the stretch test.*

Material and Methods. During the cadaveric study on 7 specimens 7–20 h after death, strain deformation of plexus brachialis as well as compression deformation caused by the surrounding structures of the neurovascular bundle were investigated in the arm abduction position of 0°, 90°, 12°, 150°, and 180°. One nerve sample was studied histologically after 15% stretch on the bench.

Results. The relative strain deformation of 3%–23% was documented during 0° to 180° abduction tests. The strain deformation from 0° to 90° was significant (P<0.001). The mean pressure change in the bundle was 13.6 mm Hg at 90°, 53.7 mm Hg at 120°, 73.4 mm Hg at 150°, and 89.0 mm Hg at 180° arm abduction. An increase in pressure was significant in the intervals: 0°–90° (P<0.001), 91°–120° (P<0.001), 121°–150° (P<0.001) and 151°–180° (P<0.05).

Conclusions. Nerve traction and tissue compression arising during the arm abduction above 90° were found to be sufficient to induce lesions in neural bundles of the plexus brachialis.

Introduction

Postoperative upper extremity neuropathy remains a serious anesthetic problem and often it has a close relationship with patient's position. The real incidence of postoperative neuropathies that are not related to regional anesthesia is unknown because they may be transitory and last only some hours or days and therefore are not recorded in a medical card. We can judge about the incidence of postoperative neuropathies from some sources (1, 2), and their incidence is estimated to be 0.1% of all anesthesia cases and 0.04% accounts for ulnar neuropathy (3, 4). According to the analysis of the American Society of Anesthesiologists' (AS) Closed Claims Study in 1990, peripheral nerve injury accounts for 15% of all submitted complaints about postoperative complications (5). Data from the ASA Closed Claims Study gathered in 1994 about the period from 1970 to 1994 indicate that the percentage of peripheral postoperative neuropathies remains constant – 15%–18% of all claims despite increasing safety requirements during anesthesia (6). According to the opinion of insurance companies, the claims made up approximately one-tenth of real numbers of complications because one part of damages regresses completely, and direct reconciliation about compensation of the other part was found (4).

Among all nerve injuries, *n. ulnaris* is the most frequently injured (28%) following by the *plexus brachialis* (20%), roots of *plexus lumbosacralis* (16%), and the spinal cord (13%) (7).

Strain, compression, or direct damage to a nerve caused by surgical and anesthetic manipulations may lead to postoperative neuropathy. In this study, the parameters of strain and compression during arm abduction were more deeply investigated. External forces that cause compressions are known (8) but pressures that rise in a neurovascular bundle and in the surrounding soft tissues in the cervico-costoclavicular-axillary area have not been studied yet. Limits of nerve strain up to beginning of pathological changes have also been investigated in vivo studies on animals (9, 10), but there are no data on a degree of strain deformation in human during arm abduction.

The aim of our study was to clarify the role of different mechanisms in nerve injury during arm abduction positions.

The tasks were to measure pressures in a neurovascular bundle in the cervico-costoclavicular-axillary area, determine the strain deformation of the

Correspondence to E. Vasilevskis, Riga Hospital No. 2, Gimnastikas iela 1; 1004 Riga, Latvia
E-mail: edgars.vasilevskis@inbox.lv

plexus brachialis and peripheral nerves during arm abduction, and evaluate the histological changes of nerve after the stretch test comparable with arm position-induced stretch during the surgery.

Material and Methods

The experiments were carried out in the State Forensic Medicine Center using a postmortem material of 7 cadavers. Strain deformation of *plexus brachialis* and compression were investigated in the arm abduction position of 0°, 90°, 120°, 150°, and 180°. After the approval of the Riga Stradins University Ethics Committee, the study was carried out in the State Forensic Medicine Centre. In the study, cadaveric material was taken before autopsy. Death occurred 7–20 hours before the beginning of autopsy. The study had 3 stages.

During the first stage of the study, strain deformation of the peripheral nerves of *plexus brachialis* at the level of *sulcus bicipitalis* was investigated. First, a neurovascular bundle was prepared in the middle third of the humerus, and *nervus medianus*, *nervus ulnaris* and in one case, *nervus cutaneus brachii superficialis* were dissected as well. Each of the separated nerves was manually transfixed with needles from outside to the muscles at two points with approximately 20–30 mm between each other depending on approach facilities. After transfixion of the nerve, the position of the arm was changed from 0° to 90°, 120°, 150°, and 180° abduction. Photographing method was used for determination of changes in the length of nerve segment in every abduction position and analyzed by the AutoCAd software (AutoCAD 2010, France).

During the second stage of the study, an original method using an angioplasty catheter and measuring changes of pressure in its dilatation balloon was used for determination of the deformation pressure of neurovascular bundle. For this purpose, *v. brachialis* in the dissected *sulcus bicipitalis* was catheterized. An angioplasty catheter balloon (Fox plus, Abbott) was used with a dilatation cylinder 40 mm in length and 12 mm in diameter when inflated. Selected diameter of the balloon complies with a mean distance between the first rib and the clavicle as well as with a diameter of *v. subclavia* during inspiration (11–13). The catheter was initially introduced up to the attachment site of *mm. scaleni* to the clavicle. This distance was determined before the beginning of measurements with the arm abducted at 90° by measuring distance between the expected introduction site of the catheter in vein and a point above the junction of the clavicle with *mm. scaleni*. The catheter with a trident was attached to a pressure manometer (model Keyence AP-30, Japan), and the balloon was inflated with air up to the level of 20 kPa (150 mm Hg) or initial diameter of 12 mm. Then, changes in pressure in the catheter balloon were recorded changing arm position. The changes in pressure present a pressure of surrounding tissues. Measurements were performed on both hands for 5 times pulling back the balloon each time for 3 cm while the level of humeral head was achieved. The maximal change of pressure was used in the analysis.

During the third stage of the study, an analysis of one nerve sample strain deformation was done on test bench. The fragment of *n. medianus* 7 cm in length was dissected; 2 cm were used as a comparative material. The remaining 5 cm were inserted in the test bench with an inner distance of 30 mm. After fixation of the nerve, the fragment was extended for 15% or 4.5 mm as such deformation was also observed in the first stage of our study, and 15% relative deformation seemed to cause a significant decrease in compound motor action potentials (CMAP) (9), but 11%–18% tractions stopped microcirculation and arterial extrafascicular blood supply (8) that could cause nerve injury. Maintaining this stretching, the nerve sample was immersed into cell-stabilizing Custodiol solution for 3 hours. The stretch of 15% was chosen because several measurements of our study exceeded this limit, and in a study by Brown et al. (9), this decreased the CMAP with further development of neuropathies. After 3 hours, the nerve was placed into glutaraldehyde solution for further analysis.

Electron Microscopy. Tissue samples were fixed in 2.5% glutaraldehyde. For transmission electron microscopy (TEM), the samples were postfixed in 1% osmium tetroxide, dehydrated through a graded ethanol series, and embedded in Epon epoxy resin. Ultrathin sections (70–80 nm in thickness) were cut with a LBR ultramicrotome, collected on formvar-coated grids, double stained with uranyl acetate and lead citrate, and examined with a JEM 1011 electron microscope.

For scanning electron microscopy (SEM), tissue dehydration was performed using increasingly concentrated solutions of acetone (70%, 80%, 90%, and 99.9% acetone in water, change every 10 min), dried by the critical point method using liquid CO_2, and coated with a thin layer of gold. The samples were analyzed by using a scanning electron microscope JSM-6490LV. For observation in the SEM mode, the untitled specimens were examined at an accelerating voltage of 20 kV.

Statistical Analysis. Results were summarized using descriptive statistics, and all the study data were systematized with the Microsoft Excel data processing program. The *t* test was used for statistical processing with the program PASW Statistics 18.0. Confidence limit was set at alpha 0.05. The study included measurements obtained from only 7 ca-

davers as more material during the planned study period was not available, and the data obtained showed already an explicit and interpretable trend.

Results

Strain Deformation. The relative strain deformation of 3%–23% was recorded during the 0° to 180° abduction tests. The mean relative nerve strain deformation was found to be 6.37% at 90° arm abduction, 6.76% at 120°, 7.6% at 150°, and 7.76% at 180° abduction (Fig. 1). The absolute deformation of the nerve segment was from 29.3 mm to 31.57 mm (Fig. 2). In separate cases (measurements 1, 2, and 5), arm position of 180° could not be achieved due to cadaverous stiffness.

The most significant strain deformation of the nerve segment during arm abduction was observed at 0° to 90° angle, and this change was significant ($P<0.001$), whereas further arm abduction to 120°, 150°, and 180° caused less significant relative deformation; however, the changes arising from the position of 90° to 180° were still statistically significant ($P<0.05$).

Pressure Measurements. Changes in pressure in a neurovascular bundle and in the surrounding soft tissues during different arm positions were measured in absolute values; however, only relative pressure changes in the dilatation balloon were analyzed.

Measurements were made in kPa, but then conversion to mm Hg was done. The mean changes in pressure in dilatation balloon catheter that was further transmitted to the surrounding tissues increased from 20.22±0.33 kPa (153.7±2.5 mm Hg) at 0° to 22.01±1.45 kPa (167.3±11.0 mm Hg) at 90° abduction, 27.19±3.17 kPa (206.7±24.1 mm Hg) at 120° abduction, 29.88±4.03 kPa (227.1±30.6 mm Hg) at 150° abduction, and 31.94±5.29 kPa (242.7±40.2 mm Hg) at 180° abduction. The absolute mean changes in pressure generated in the balloon were 1.79 kPa (13.6 mm Hg) at 90°, 7.07 kPa (53.7 mm Hg) at 120°, 9.66 kPa (73.4 mm Hg) at 150°, and 11.72 kPa (89.0 mm Hg) at 180° arm abduction (Fig. 3). An increase in pressure was significant in the intervals: 0°–90° ($P<0.001$), 90°–120° ($P<0.001$), 120°–150° ($P<0.001$), and also 150°–180° ($P<0.05$) (Fig. 3).

Electron Microscopy Results. Transmission Electron Microscopy. The myelinated and unmyelinated nerve fibers were studied ultrastucturally before and after tension. Before tension, some myelinated nerve fibers showed expanded spaces within the myelin layer between myelin membranes, filled with homogeneous cytosol containing mitochondria. Cytoskeleton elements were well marked and properly oriented in central axis. The numbers of myelin layers within a single nerve fiber varied greatly. Unmyelinated fibers mostly showed nerve cell processes:

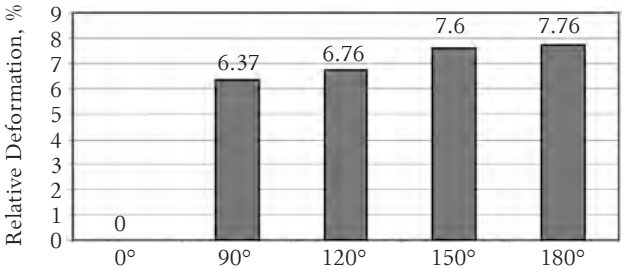

Fig. 1. Relative strain deformation of the nerves during abduction tests

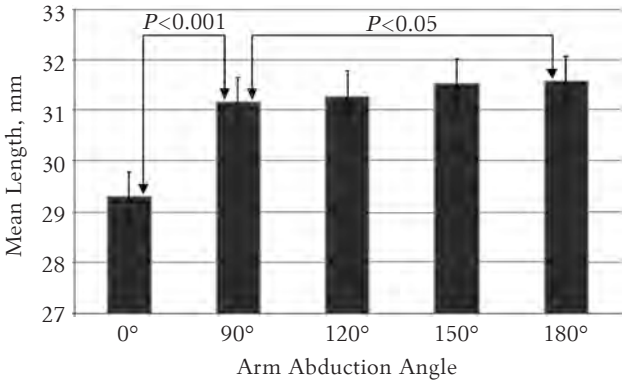

Fig. 2. Strain deformation of the nerves during abduction tests

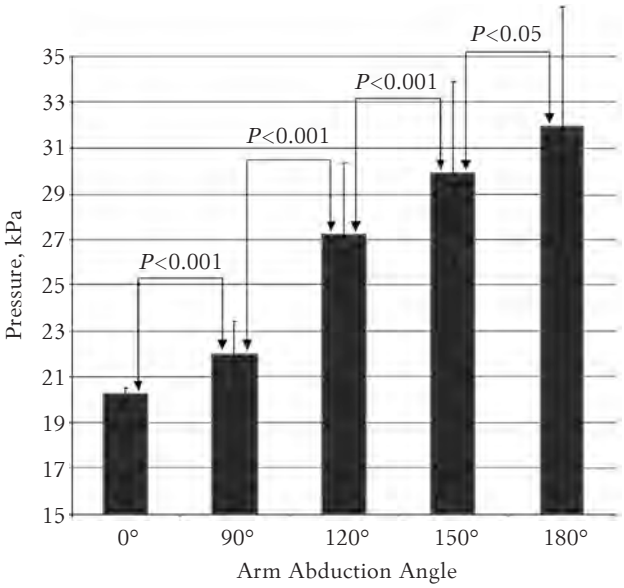

Fig. 3. Changes in pressure in the cervicobrachial neurovascular bundle

swelling and mitochondrial degeneration. Microtubules were oriented mostly parallel to the long axis of the nerve fiber. Collagen fibers were observed to be tightly associated with the basement membrane of myelinated nerve fibers (Fig. 4 A and B).

Disruption of myelin sheets was demonstrated after the specimen tension. Electron micrographs revealed straightening of myelinated and unmyelinated nerve fibers and surrounding collagen fibers.

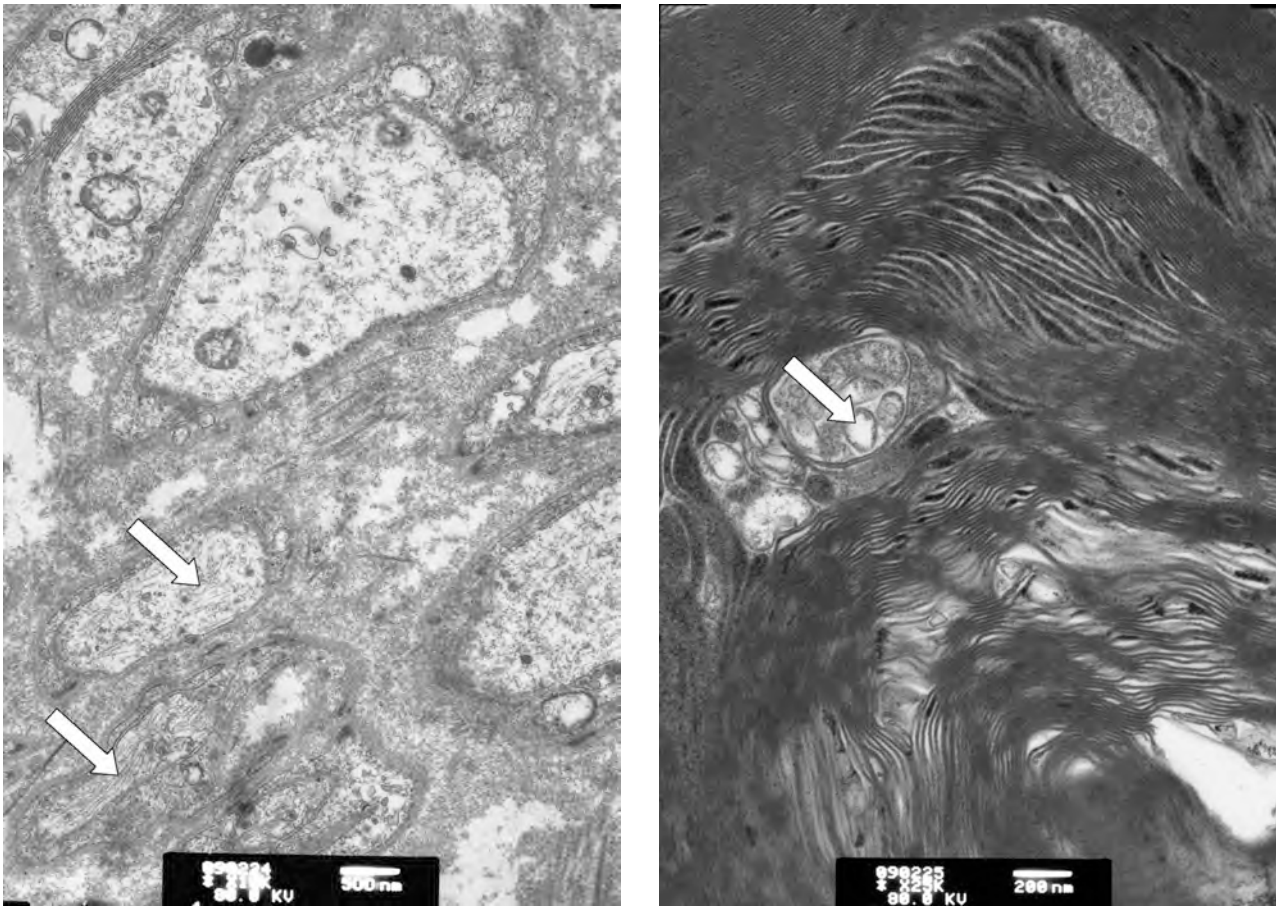

A B

Fig. 4. Structure of the nerve fibers before application of tension

A, Transmission electron micrographs demonstrate nerve cell processes filled with homogeneous cytoskeleton elements (arrows) (original magnification ×25000); B, some nerve fibers before tension demonstrate irregularly expanded spaces between myelin membranes, filled with cytosol and swollen mitochondria (arrow) (original magnification ×10000).

The cross-sections of unmyelinated nerve fibers were elliptically shaped and showed swollen cytoplasm and a slight decrease in the number of cytoskeleton elements (Fig. 5 A and B).

Scanning Electron Microscopy. Large and small nerve fibers arranged in compact bundles were observed by the use of SEM before tension. These nerve bundles were surrounded by collagen fibers. Larger bundles of nerve fibers were enveloped by denser connective tissue (Fig. 6 A).

The nerve fibers became enlarged after application of tension, often having a flattened and ribbon-like external appearance. A significant number of nerve fibers were disrupted, and the connective tissue was partly damaged (Fig. 6 B).

Discussion

To date, no published data on directly measured transmural pressure change in human brachial nerve-vascular bundle and in the surrounding soft tissue during the arm movements are available, because all the pressure measurements are usually done outside the limb. Moreover, there are few publications about the human nerve tensile deformation. Cadaver and live nerve excursion studies during arm and hand movements are only available (14).

Data are available for other structurally more complex structures such as arteries and their mechanical properties after death. These studies suggest that up to 24 hours after death, the mechanical properties of soft tissues are not substantially altered (15). Consequently, our data on cadaveric tissues, which were obtained 7–20 hours after death, were comparable to tensile deformation of a live nerve and live surrounding tissue pressure on the nerve-vascular bundle.

Strain Deformation. Up to now, histological and electrophysiological changes of peripheral nerves during in vivo and in vitro strain have been thoroughly examined. Conversely, there are rather controversial data about a threshold of strain deformation that results in functional changes. Data about the pathology vary from 11% to 25% and even 100%

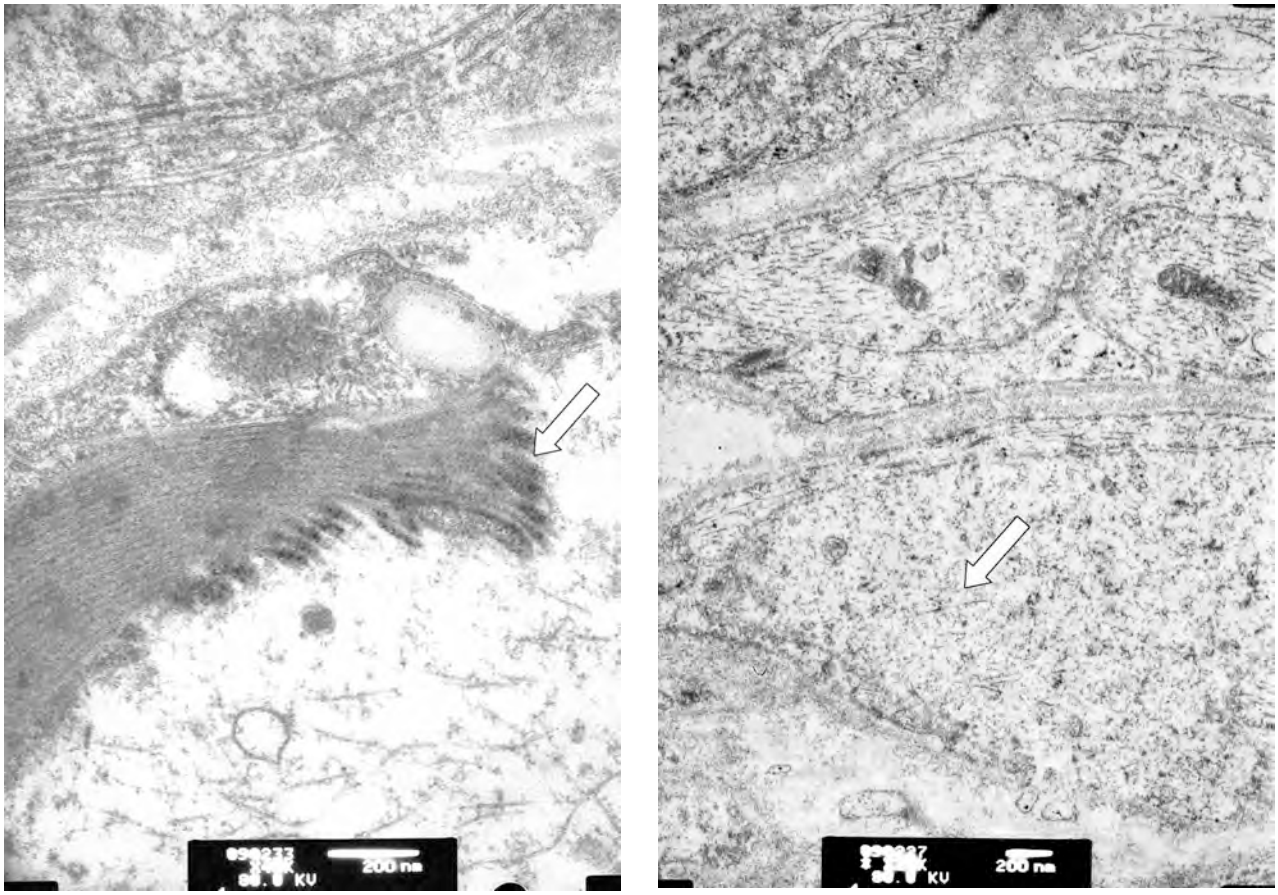

A **B**

Fig. 5. Electron micrographs after application of tension for 3 hours
A, disrupted myelinated nerve fibers are present (arrow) (original magnification ×40000); B, unmyelinated nerve fiber with swollen cytoplasm (arrow) (original magnification ×20000).

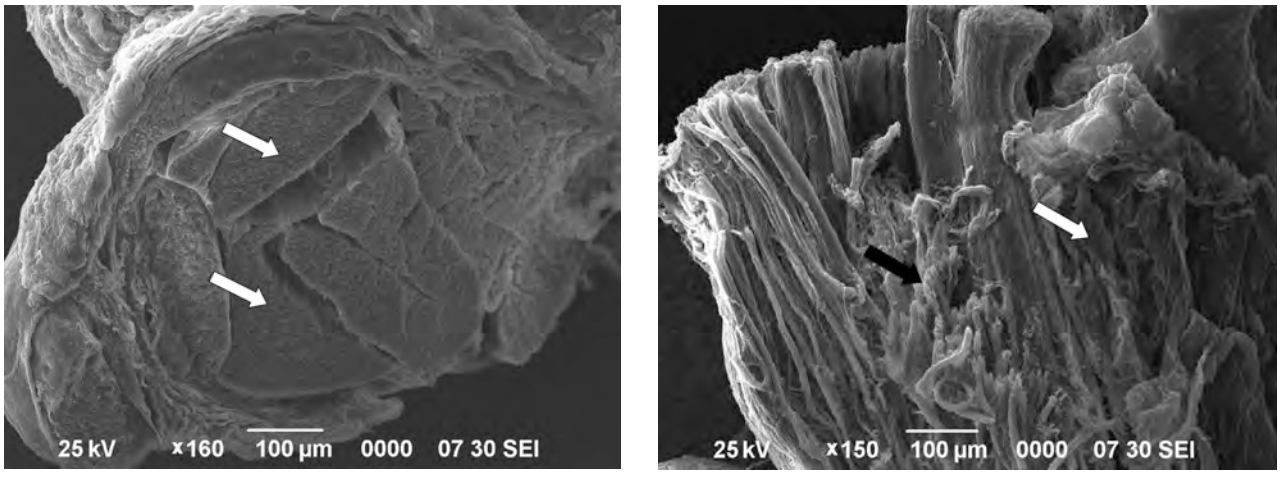

A **B**

Fig. 6. Scanning electron micrographs before and after tension
A, cross-section of peripheral nerve fiber before application of tension shows compact arrangement of fibers (arrows) (original magnification ×160); B, after tension, abnormal surfaces of nerve fibers are revealed (white arrow), and myelinated nerve fibers are destroyed (black arrow) (original magnification ×150).

peripheral nerve strain deformation (16). Although the data are rather controversial, a relative deformation of 15% seems to cause a significant decrease in compound evoked motor potentials (CEMP) that further leads to permanent tissue changes in the form of neuropraxia (9). A nerve flexibility threshold is achieved at 20% and becomes critical at 30% (17). Whereas, investigations on blood supply of the nerve have determined that 5%–10% traction stops venous flow and 11%–18% tractions stop microcirculation and arterial extrafascicular blood supply (8). However, this applies to laboratory animals. In our study, we tried to clarify what is strain deformation of the human neural tissues. Relative deformation for abduction from 0°–180° was observed in a wide diapason ranging from 3% to 23%. It suggests that there are marked individual features of the neural tissue strain, and a physiological traction reserve of the limb that could be exceeded is not well known. A different degree of strain of the neurovascular bundle was observed also macroscopically after dissection with the arm in abduction position. That could explain the low relative deformation of nerve in some tests.

Plexus brachialis is fixed to the paravertebral fascia in the cervical area and to the axillary fascia in the axilla (2). Further, nerves divide and do not function as a one unit anymore. We measured strain of the peripheral nerves in the upper arm during arm abduction; however, it has been determined that it does not present an equal deformation along all nerve axons, and the plexus seems to be deformed more than separate peripheral nerves (13).

Electron Microscopy Data. Our study has demonstrated that tension of peripheral nerve may induce significant ultrastructural changes, endangering the normal integrity of the nerve. Nerve length probably has been changed due to tensile stress that may induce ultrastructural changes of peripheral nerves (18). The changes found to be induced by tension were swelling of unmyelinated nerve fibers, swelling of mitochondria and disorganization of their cristae. Ultrastructural findings suggested that under exposure of strain applied for 3 hours, unmyelinated nerve fibers were more vulnerable compared with myelinated ones. The normally circumferential outline of the myelin sheath was changed to irregular-shaped profiles; however, alterations in the myelin layer were not noticed. Under experimental conditions used in the present study, our ultrastructural data are in line with the results reported by Dyck et al. (19) in case of nerve compression.

The present data did not allow observing a decrease in myelin sheet thickness due to the applied tension; however, the breakage of myelin sheet was observed. The action of mechanical forces on peripheral nerves can give rise to neurodegeneration reported by Burnett and Zager (20) as well as Pham and Gupta (21).

Nerve Compression. Most of the compression studies analyze tourniquet effect on the peripheral nerves (22), but there are no data about the compression on the whole neural plexus above the axilla.

As the result of direct pressure, an effect on characteristic paranodular demyelinization at the compression site is observed (23). At the same time, the microcirculation changes of the nerve that lead to ischemia are also observed: 40–50 mm Hg causes an impairment in the arteriolar and intrafascicular capillary flow (8). Pressures recorded by us were lower than the mean physiological systolic pressure, but they were in the range to significantly affect the microcirculation. Of course, exposition time should be taken into account. A recently published study (24) has demonstrated that the bilateral damage of *plexus brachialis* was explained only by nerve stretching in 90° arm abduction position lasting 12 hours.

Anatomy of the investigated area of our study is most researched in association with thoracic outlet syndrome. A series of studies have determined the narrowest areas of the *plexus bronchialis* neurovascular bundle between *mm. scaleni* and axilla. The mean parameters for healthy population are also established by computed tomography (CT) and magnetic resonance imaging (MRI) (11, 12). Three main compression points are also determined: *mm. scaleni* attachment site to the first rib, area between the first rib and the clavicle, and the canal below *m. pectoralis* major tendon. In these points, pressure increased more during the provocation tests. It is important to remember that arm abduction and shoulder lowering belong to these provocation tests, and making provocation tests in a patient without thoracic outlet syndrome may also reveal some degree of neurovascular compression (25). Separately from the thoracic outlet syndrome, the forth neurovascular compression point – the humeral head – is described in literature (1–4, 26); however, it has not been documented by angiography, MRI, or CT examinations.

An answer to the question whether some patients are more predisposed to the development of neuropathy is partly provided by the "double crush" and "reverse double crush" theories. If the nerve axon is already changed or if general trophic condition of the nerves is disturbed, e.g., in the case of diabetes, chronic renal failure, or denutrition, the risk significantly increases (27, 28).

After extensive research from the 1960s to the 1970s, the tourniquet time is being recorded during every operation since it may limit the risk of ischemia. The same recording could be useful for the arm position marking the abduction degree and exposition time.

Conclusions

Strain deformation was found in more than 6% at 90° and 120° and more than 7% at 150° and 180° arm abduction and could be the cause of postoperative neuropathy. The absolute pressure detected during the section in the neurovascular bundle and surrounding soft tissue with the frequent arm abduction positions during surgery was 53.7 mm Hg at 120° and 73.4 mm Hg at 150°. These tissue pressures arising during the neural traction and hand abduction above 90° were found to be sufficient to create the compression on the neural bundles of the *plexus brachialis*. The histological changes after 15% nerve strain deformation during 3 hours on the test bench confirmed significant nerve tissue injury.

Statement of Conflict of Interest

The authors state no conflict of interest.

References

1. Parks BJ. Postoperative neuropathies. Surgery 1993;71: 348-57.
2. Britt BA, Gordon RA. Peripheral nerve injuries associated with anesthesia. Can Anaesth Soc J 1964;11:514-24.
3. Warner MA, Warner ME, Martin JT. Ulnar neuropathy. Incidence, outcome, and risk factors in sedated or anesthetized patients. Anesthesiology 1994;81:1332-40.
4. Drizenko A, Scherpereel Ph. Manuel des positions opératoires en anésthesie. Paris: Editions Pradel; 1997. p. 20-3.
5. Keats AS. The closed claims study. Anesthesiology 1990;73: 199-201.
6. Cheney FW, Domino KB, Caplan RA, Posner KL. Nerve injury associated with anesthesia: a closed claims analysis. Anesthesiology 1999;90(4):1062-9.
7. Kroll DA, Caplan RA, Posner K, Ward RJ, Cheney FW. Nerve injury associated with anesthesia. Anesthesiology 1990;73(2):202-7.
8. Rydevik B, Lundborg G, Bagge U. Effects of graded compression on intraneural blood blow. An in vivo study on rabbit tibial nerve. J Hand Surg Am 1981;6(1):3-12.
9. Brown R, Pedowitz R, Rydevik B, Woo S, Hargens A, Massie J, et al. Effects of acute graded strain on efferent conduction properties in the rabbit tibial nerve. Clin Orthop Relat Res 1993;(296):288-94.
10. Singh A, Kallakuri S, Chen C, Cavanaugh JM. Structural and functional changes in nerve roots due to tension at various strains and strain rates: an in-vivo study. J Neurotrauma 2009;26(4):627-40.
11. Chang CS, Chuang DC, Chin SC, Chang CJ. An investigation of the relationship between thoracic outlet syndrome and the dimensions of the first rib and clavicle. J Plast Reconstr Aesthet Surg 2011;64(8):1000-6.
12. Adesanya O. Thoracic outlet syndrome secondary to first rib anomaly: the value of multi-slice CT in diagnosis and surgical planning. Ir Med J 2007;100(2):377.
13. Gómez E, Bastida R, Oleaga L, Gorriño M, Grande D. [Diagnosis of thoracic outlet syndrome by angio-MRI]. Radiologia 2006;48(5):295-300.
14. McLellan DL. Letter: Longitudinal sliding of median nerve during hand movements: a contributory factor in entrapment neuropathy? Lancet 1975;15;1(7907):633-4.
15. Patel DJ, Tucker WK, Janicki JS. Dynamic elastic properties of the aorta in radial direction. J Appl Physiol 1970;28(5): 578-82.
16. Mitchell SW. Injury of nerves and their consequences. Philadelphia: Lippincott; 1872.
17. Sunderland S, Bradley K C. Stress strain phenomena in denervated peripheral nerve trunks. Brain 1961;84:125-7.
18. Topp KS, Boyd BS. Structure and biomechanics of peripheral nerves: nerve responses to physical stresses and implications for physical therapist practice. Phys Ther 2006;86(1): 92-109.
19. Dyck PJ, Lais AC, Giannini C, Engelstad KJ. Structural alterations of nerve during cuff compression. Proc Natl Acad Sci U S A 1990;87(24):9828-32.
20. Burnett MG, Zager EL. Pathophysiology of peripheral nerve injury: a brief review. Neurosurg Focus 2004;16(5):E1.
21. Pham K, Gupta R. Understanding the mechanisms of entrapment neuropathies. Neurosurg Focus 2009;26(2):E7.
22. Nitz AJ, Dobner JJ, Matulionis DH. Structural assessment of rat sciatic nerve following tourniquet compression and vascular manipulation. Anat Rec 1989;225(1):67-76.
23. Ochoa J, Fowler TJ, Gilliatt RW. Anatomical changes in peripheral nerves compressed by a pneumatic tourniquet. J Anat 1972;113(Pt 3):433-55.
24. Hida A, Arai T, Nakanishi K, Nagaro T. Bilateral brachial plexus injury after liver transplantation. J Anesth 2008; 22(3):308-11.
25. Ozoa G, Alves D, Fish DE. Thoracic outlet syndrome. Phys Med Rehabil Clin N Am 2011;22(3):473-83, viii-ix.
26. Samii K. [Surgical anesthesia and intensive care]. [In French]. 2nd ed. Paris: Médecine-Sciences Flammarion; 1995. p. 492-500.
27. Schmid AB, Coppieters MW. The double crush syndrome revisited – a Delphi study to reveal current expert views on mechanisms underlying dual nerve disorders. Man Ther 2011;16(6):557-62.
28. Moghtaderi A, Izadi S. Double crush syndrome: an analysis of age, gender and body mass index. Clin Neurol Neurosurg 2008;110(1):25-9.

Received 6 September 2010, accepted 31 October 2011